ACS APPLIED MATERIALS & INTERFACES

Research Article

www.acsami.org

Peptide-Bridged Assembly of Hybrid Nanomaterial and Its Application for Caspase-3 Detection

Yupeng Shi,[†] Changqing Yi,*[,†] Zhaomin Zhang,[†] Heng Zhang,[†] Meijin Li,[‡] Mengsu Yang,[§] and Qing Jiang[†]

[†]Key Laboratory of Sensing Technology and Biomedical Instruments (Guangdong Province), School of Engineering, Sun Yat-Sen University, Guangzhou, China

[‡]Key Laboratory of Analysis and Detection Technology for Food Safety (Ministry of Education and Fujian Province), Department of Chemistry, Fuzhou University, Fuzhou, China

[§]Key Laboratory of Biochip Technology, Biotech and Health Centre, Shenzhen Research Institutes of City University of Hong Kong, Shenzhen, China

Supporting Information

ABSTRACT: Recent developments in the rational design and the controlled assembly of nanoscale building blocks have resulted in functional devices such as nano-optoelectronics, novel contrast probes for molecular imaging, and nanosensors. In the present study, we designed and synthesized a hybrid nanomaterial consisting of $[Ru(bpy)_3]^{2+}$-encapsulated silica nanoparticles (SiNPs) and gold nanoparticles (AuNPs) through peptide-bridged assembly in a controllable way. A peptide that contains recognition sequence DEVD specific for active caspase-3 cleavage was employed to bring SiNPs and AuNPs into close proximity through specific molecular recognition. A FRET system with SiNPs as energy donors and AuNPs as energy acceptors has been thus developed and applied for caspase-3 detection. A change in distance between the two building blocks resulted in a change in FRET efficiency, causing a ratiometric change in emission. Caspase-3 triggers the cleavage of the peptide links between the two nanoparticles and releases AuNPs from the nanohybrids, inducing the activation of SiNPs to the "ON" state. The fluorescence turn-on response is specific to caspase-3 and allows the detection of caspase-3 as low as 0.05 U mL^{-1} (~6 pM).

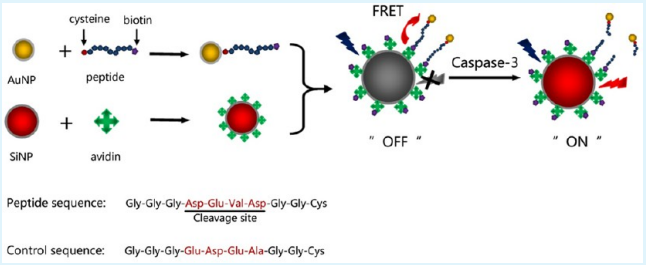

KEYWORDS: *hybrid nanomaterials, silica nanoparticles, gold nanoparticles, caspase-3, fluorescence resonance energy transfer*

INTRODUCTION

Recent developments in the rational design and the controlled assembly of nanoscale building blocks have resulted in functional devices such as nano-optoelectronics,[1−4] novel contrast probes for molecular imaging,[5−7] and nanosensors.[8−16]

Physical methods based on electrostatic interaction,[1] $\pi-\pi$ stacking interaction,[2] and hydrophobic interaction,[3] and chemical methods based on in situ mineralization,[4] covalent bonds,[15] and inorganic scaffolds[17] have all been demonstrated to successfully construct hybrid nanomaterials.[18] However, many challenges are still present in the rational design of functional nanoscale structures, where novel physical and chemical methods are required to address the issues such as nonspecificity, low selectivity, and uncertainty of functionalization positions.[18] Biomolecules are ideal candidates in directing the rational design of functional nanodevices because of their capabilities to self-assemble into a wide variety of organized and complicated nanostructures with high specificity and efficiency. The prototypical biomolecules include proteins,[19,20] DNA/RNA molecules,[21−24] and virus/microorganisms.[25−28] Proteins can act as templates or scaffolds to construct nanoscale architectures[19] or serve as linkers to assemble functional nanohybrids.[20] Taking advantages of its sequence specific hybridization, DNA/RNA molecules have been demonstrated to be versatile nanoscale building blocks for assembling functional 1D and 3D architectures.[21−24] Microorganisms, such as virus,[25,26] bacteria,[27] and diatom,[28] have been employed as scaffolds for organizing nanocomponents into complicated 3D structures. Because it integrates the self-assembly with biological events,[29] biomolecule-directed strategy shows promising applications especially in bioanalysis and biodection. In addition, the distance and strength between the nanoscale building blocks may be controlled and specifically designed in the resulting architectures through manipulating the bridging biomolecules.

Therefore, interests in utilizing biomolecules to create hybrid nanomaterials-based sensors and probes continue to grow relatively unabated.[5−16] Special attention has been paid to the

Received: January 8, 2013
Accepted: June 27, 2013
Published: June 27, 2013

Scheme 1. Schematic Principle of Caspase-3 Detection by Using the SiNP-peptide-AuNP Conjugates As Nanoprobes

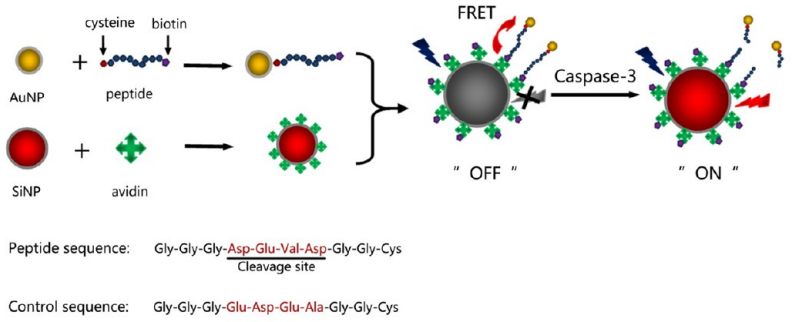

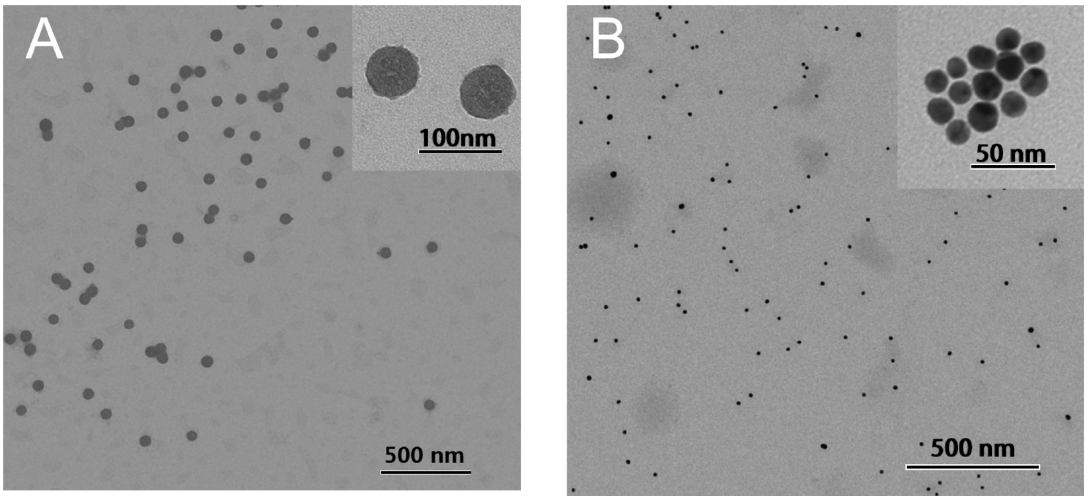

Figure 1. TEM image of carboxylated $[Ru(bpy)_3]^{2+}$-encapsulated (A) SiNPs and (B) AuNPs.

nanoprobes and nanosensors based on fluorescence resonance energy transfer (FRET), where non-radiative energy transfer via long-range dipole−dipole interactions depend on the distance-between energy donors and acceptors.[30] To improve FRET efficiency for obtaining better analytical performance, it is of continuing interest to optimize FRET models through looking for new energy donor−acceptor pairs.[8] Recently, nanoscale fluorescence energy donors such as semiconductor quantum dots (QDs)[9,13−16] and upconversion luminescent nanoparticles (UCN),[8,10−12] and nanoscale energy acceptors such as gold nanoparticles (AuNPs),[13−16] graphene oxide (GO),[8,9,12] and carbon nanoparticles (CNPs)[10,11] have been successfully assembled to develop FRET-based nanosensors for the detection of glucose,[8] DNA,[9] proteins,[10,11,13,16] mycotoxins,[12] and inorganic ions.[14,15] Among available nanoscale fluorescence energy donors, $[Ru(bpy)_3]^{2+}$-encapsulated silica nanoparticles (SiNPs) are an appealing choice because of their high luminescence quantum yield, good photostability, and bio-compatibility.[31] When interfaced with biomolecules including proteins, peptides, and DNA, the resulting SiNP-based nanocomposites are extensively applied in bioanalysis and biomedical research such as disease diagnosis, drug screening, and cellular imaging.[31−33]

In the present study, we designed and synthesized the hybrid nanomaterial consisting of $[Ru(bpy)_3]^{2+}$-encapsulated SiNPs and AuNPs through peptide-bridged assembly in a controllable way, as depicted in Scheme 1. A peptide which contains recognition sequence DEVD specific for active caspase-3 cleavage was employed to bring SiNPs and AuNPs into close proximity through specific molecular recognition.[34] A FRET system with SiNPs as energy donors and AuNPs as energy acceptors has been thus designed and applied for caspase-3 detection. A change in distance between the two building blocks resulted in a change in FRET efficiency, causing a ratiometric change in emission. Caspase-3 triggers the cleavage of the links between the two nanoparticles and releases AuNPs from the nanohybrids, inducing the activation of SiNPs to the "ON" state. The fluorescence turn-on response is specific to caspase-3 and allows the detection of caspase-3 as low as 0.05 unit mL^{-1} (~6 pM).

RESULTS AND DISCUSSION

Synthesis and Functionalization of SiNPs and AuNPs. Fairly uniform carboxylated $[Ru(bpy)_3]^{2+}$-encapsulated SiNPs were prepared by using a water-in-oil reverse micelle method.[35] TEM images (Figure 1A) clearly showed that the SiNPs were dispersed very well in aqueous solutions, spherical in shape with a diameter of ~50 nm, and no aggregation was observed. Dynamic light scattering (DLS) measurements revealed that the diameter of SiNPs was 46.46 nm (Table 1), which was

Table 1. Average Diameter and Zeta-Potentials of Nanocomponents in Ultra Pure Water

	zeta potential (mV)	size (nm)
SiNPs	−38.4	46.46
SiNP-avidin	−16.4	112.44
AuNPs	−34.2	12.58
AuNP-biotinylated peptides	5.7	14.10

dx.doi.org/10.1021/am401935y | ACS Appl. Mater. Interfaces 2013, 5, 6494−6501

consistent with the TEM observations. The further functionalization of SiNPs with avidin were carried out using carbodiimide chemistry, where cross-linking reactions between free carboxylic groups of SiNPs and amine groups on avidin were initiated by adding a solution of EDC and NHS.[36] Surface modification of SiNPs with avidin resulted in the aggregation of SiNPs to some extent, as evidenced by TEM images (see Figure S1A in the Supporting Information) and the average size of SiNPs changing from 46.46 to 112.44 nm (Table 1). The change of zeta potential of SiNPs before and after surface modification from −38.4 to −16.4 mV provided an indirect evidence for the successful conjugation of avidin onto SiNPs, because avidin is positively charged in pH 7.4 assay buffer.

AuNPs were obtained by the citrate reduction of chloroauric acid.[22,37] Figure 1B displays a typical TEM image of AuNPs, where AuNPs were regular, monodisperse, and spherical in shape with a diameter of ∼13 nm. DLS measurements are consistent with the TEM observation, confirming that the diameter of as-prepared AuNPs was 12.58 nm (Table 1). Biotinylated peptides were further functionalized onto AuNPs via the Au−S bonds (see Figure S1B in the Supporting Information).[38] Because DLS measures the hydrodynamic diameter of particles in solution, the diameter of the AuNPs should be increased by the conjugated peptides.[39] DLS measurements did reveal that the size of AuNPs changed from 12.58 nm to 14.10 nm, indicating that the conjugated biotinylated peptides contributed 1.5 nm to the overall diameter. Similarly, because positively charged peptides replace the negatively charged citrate ions during the functionalization process, the zeta potential of AuNPs changed from −34.2 mV to +5.7 mV after the conjugation of biotinylated peptides (Table 1), confirming the successful conjugation of peptides onto AuNPs.

The UV−vis absorption spectra of a suspension of the $Ru(bpy)_3^{2+}$-doped SiNPs and $Ru(bpy)_3^{2+}$ in aqueous solution are shown in Figure 2. The $Ru(bpy)_3^{2+}$-doped SiNPs showed

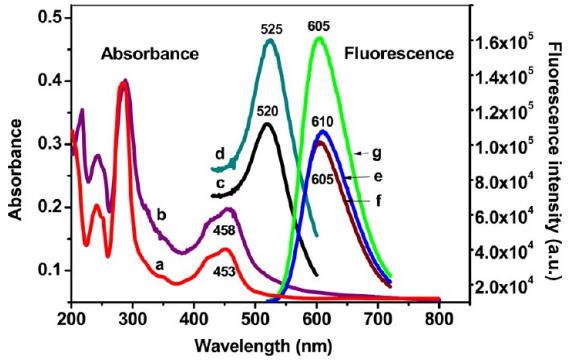

Figure 2. The UV−vis absorption spectrum of (a) $Ru(bpy)_3^{2+}$, (b) carboxylated $[Ru(bpy)_3]^{2+}$-encapsulated SiNPs, (c) AuNPs, and (d) biotinylated peptide-conjugated AuNPs; and (e) emission spectrum $Ru(bpy)_3^{2+}$, (f) carboxylated $[Ru(bpy)_3]^{2+}$-encapsulated SiNPs, and (g) avidin-functionalized SiNPs.

UV−vis absorption bands at ca. 289 and 458 nm as $Ru(bpy)_3^{2+}$ solution, attributed to the intra-ligand (IL) and the metal-to-ligand charge transfer (MLCT) transitions of the $Ru(bpy)_3^{2+}$,[32] respectively, indicating the successful incorporation of the $Ru(bpy)_3^{2+}$ in the SiNPs. The emission spectra of the $Ru(bpy)_3^{2+}$-doped SiNPs with and without avidin modification, and $Ru(bpy)_3^{2+}$ in aqueous solution are also shown in Figure 2. The $Ru(bpy)_3^{2+}$-doped SiNPs gave rise to a strong emission originating from the characteristic emission of the $Ru(bpy)_3^{2+}$. Compared to the $Ru(bpy)_3^{2+}$ in aqueous solution, the $Ru(bpy)_3^{2+}$-doped SiNPs showed a slight blue shift of ca. 5 nm in the emission wavelength, possibly due to the presence of anionic surfactant.[32] The above results strongly suggested that silica encapsulation of ruthenium(II) complexes does not appear to perturb their core optical properties.

The optical properties of AuNPs were examined by UV-Vis absorption spectra. As shown in Figure 2, a characteristic surface plasmon resonance (SPR) peak is located at 520 nm, which is in agreement with the value reported in the literature.[40] Conjugation of biotinylated peptides onto AuNPs resulted in a slight red shift of ca. 5 nm in the SPR peak, possibly due to a dielectric monolayer of thiols around AuNPs.[41] No aggregation was observed, either visually (see Figure S1B in the Supporting Information) or spectrometrically (Figure 2), indicating good stability and dispersity of the biotinylated peptides modified AuNPs.

Assembly of the SiNP-peptide-AuNP Nanohybrid. Assembly of the designed hybrid nanomaterial was achieved through the highly specific biomolecular recognition of avidin-biotin. The assembled nanohybrid of SiNP-peptide-AuNP was characterized by TEM. As demonstrated in Figure 3A−C, AuNPs were successfully conjugated to SiNPs to assemble "satellite"-shaped architecture, which have also been assembled using AuNPs with different diamters.[23,37] It can be calculated on the basis of the simple geometry that one SiNP can be conjugated by a maximum of 15 14 nm AuNPs, which is consistent with the assembled "satellite"-shaped structures (insets of Figure 3B, C).

AuNPs have been used as energy acceptors with high energy transfer efficiency because of their superior quenching efficiency with an effective energy transfer distance up to 20 nm in a broad range of wavelengths.[13−16] In particular, multiple energy acceptors per donor in a FRET system is expected to increase the overall energy transfer efficiency.[42,43] In the assembled nanohybrids of SiNP-peptide-AuNP, more than ten AuNPs were brought to the vicinity of one SiNP bridged by peptide (insets of Figure 3B, C), resulting in the decrease of the fluorescence intensities of SiNPs by AuNPs through non-radiative energy transfer, as demonstrated in Figure 3D. The luminescence of the SiNPs was quenched by about ca. 75% after addition of 9.5 nM of AuNPs, indicating the successful establishment of a FRET system with high energy transfer efficiency. Apart from a strong quenching effect, a red-shift in fluorescence band up to 10 nm (from 605 to 615 nm) was observed, possibly due to polarity changes of $Ru(bpy)_3^{2+}$ caused by the conjugated AuNPs.[44]

Sensing Application of the SiNP-peptide-AuNP Nanohybrid. In the assembled SiNP-peptide-AuNP nanohybrid, the distance between the two nanocomponents can be tailored through engineering the bridging molecules. This property can be utilized for developing new sensing strategies through employing FRET technology which is a distance-dependent energy transfer phenomenon. A change in distance between the two building blocks will result in a change in FRET efficiency, causing a ratiometric change in emission. Protease can recognize and cleave a specific substrate peptide, producing two separated fragments and thus changing the distance between the two ends of the peptide. It is well known that the active form of caspase-3 existing in apoptotic cells is able to specifically recognize a tetra-peptide sequence (Asp-Glu-Val-

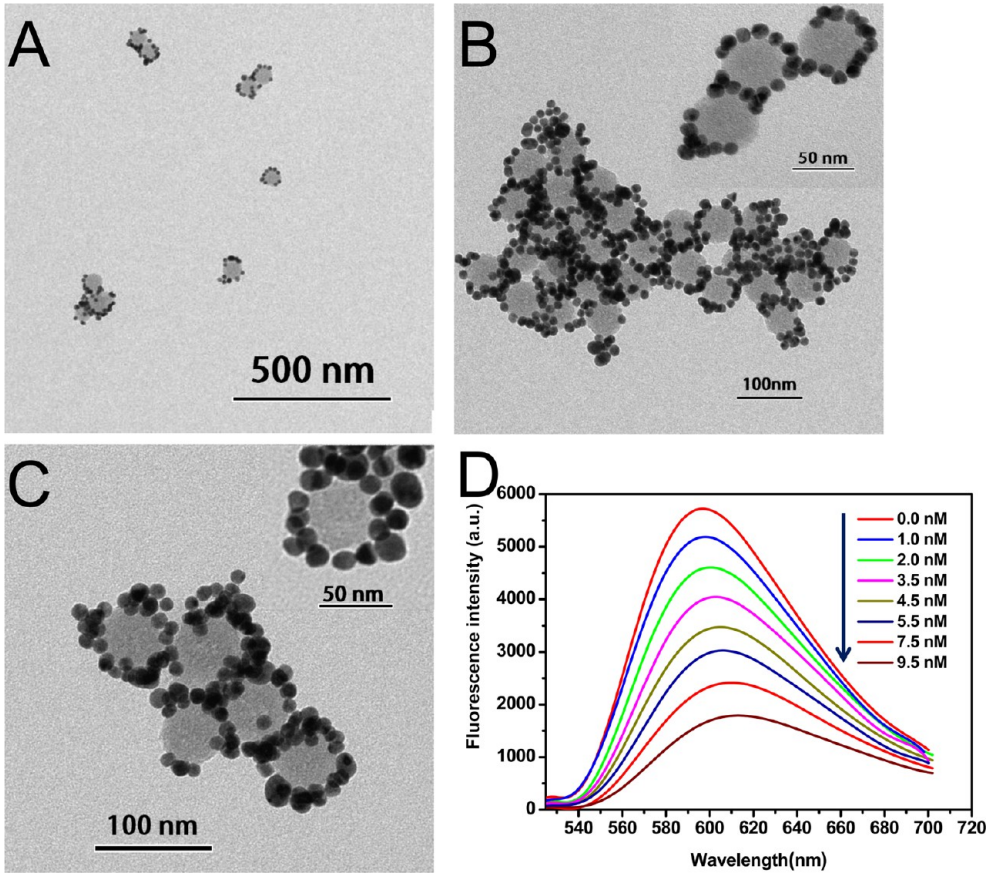

Figure 3. (A–C) TEM images of the assembled nanohybrids of SiNP-peptide-AuNP; (D) emission spectral changes of SiNPs (0.4 μg mL^{-1}) in 1 mL of 50 mM HEPES buffer solution (pH 7.4) upon addition of 13 nm AuNPs with various concentrations (0, 1.0, 2.0, 3.5, 4.5, 5.5, 7.5, and 9.5 nM).

Asp, DEVD) on peptide substrates and hydrolyze peptide bonds after the aspartic acid residues (C-terminal).[34] Therefore, it is possible to condition the assembled SiNP-AuNP nanohybrid for caspase-3 detection through tailoring the peptide to contain a specific sequence of DEVD. Caspase-3 is activated in the apoptotic cell both by extrinsic and intrinsic pathways, and has been identified as a key mediator and a well-established cellular marker of apoptosis.[45] Apoptosis is a highly regulated process of programmed cell death, which plays important roles under a variety of physiological circumstances in multicellular organisms.[46] Therefore, sensitive detection of caspase-3 activity and its inhibition by potential inhibitors is important in the development of diagnostic and therapeutic tools based on apoptosis.[47−55]

The capacity of the SiNP-peptide-AuNP for caspase-3 detection was evaluated on the basis of fluorescence intensity measurements of the nanohybrids solution at predetermined time points in the presence of 3.0 U mL^{-1} of caspase-3. Caspase-3 triggers the cleavage of the link between the two nanoparticles and releases AuNPs from the nanohybrids, inducing the activation of SiNPs to the "ON" state. As shown in Figure 4A, when caspase-3, which can specifically cleave substrate peptide DVED, was introduced into this probe system, the dramatic fluorescence recovery of the nanohybrid system was observed within 10 min. However, without caspase-3, no observable fluorescence recovery was detected for the nanohybrid system within the 360 min observation period (Figure 4A). To verify that the fluorescence recovery is a caspase-3-specific event, we carried out two critical control experiments. In the first control experiment, the caspase-3 inhibitor Ac-DEVD-CHO was added into nanohybrid system in the presence of caspase-3, resulting in the efficient blockage of the fluorescence recovery (Figure 4B). In the second control experiment, a non-target peptide linker (EDEA) was employed to assemble nanohybrids. As expected, the resultant nanohybrids showed no observable fluorescence recovery in the presence of caspase-3 (Figure 4B). Results from these two control experiments confirm that the fluorescence recovery of the nanohybrid system caused by the distance change between the two nanocomponents is indeed a caspase-3-specific event. As shown in panels C and D in Figure 4, only 0.05 unit mL^{-1} (~6 pM) of caspase-3 is able to arouse the fluorescence recovery of the nanohybrid system, and the fluorescence intensity increases gradually with the increase of the caspase-3 concentration from 0.05 to 4.0 U mL^{-1}. The fluorescence recovery linearly correlates to the concentration of caspase-3 over the range of 0.05-1.0 U mL^{-1} (inset of Figure 4D).

Previously, some interesting caspase-3 biosensors have been developed. A multiplexed assay system of proteases (matrix metalloproteinase, caspase-3, and thrombin) and their inhibition by monitoring the fluorescence change of peptide-bridged QD-AuNP nanohybrid system has been developed.[13] The fluorophore-labelled DEVD has been utilized for detection of caspase-3 activity in vivo by flow cytometry or in vitro by fluorescence measurement.[47−49] And DEVD-containing peptides were also combined with nanomaterials such as semiconductor QDs, CQDs, SiNPs, AuNPs, and GO for caspase-3 detection by colorimetric method,[50] electrochemical

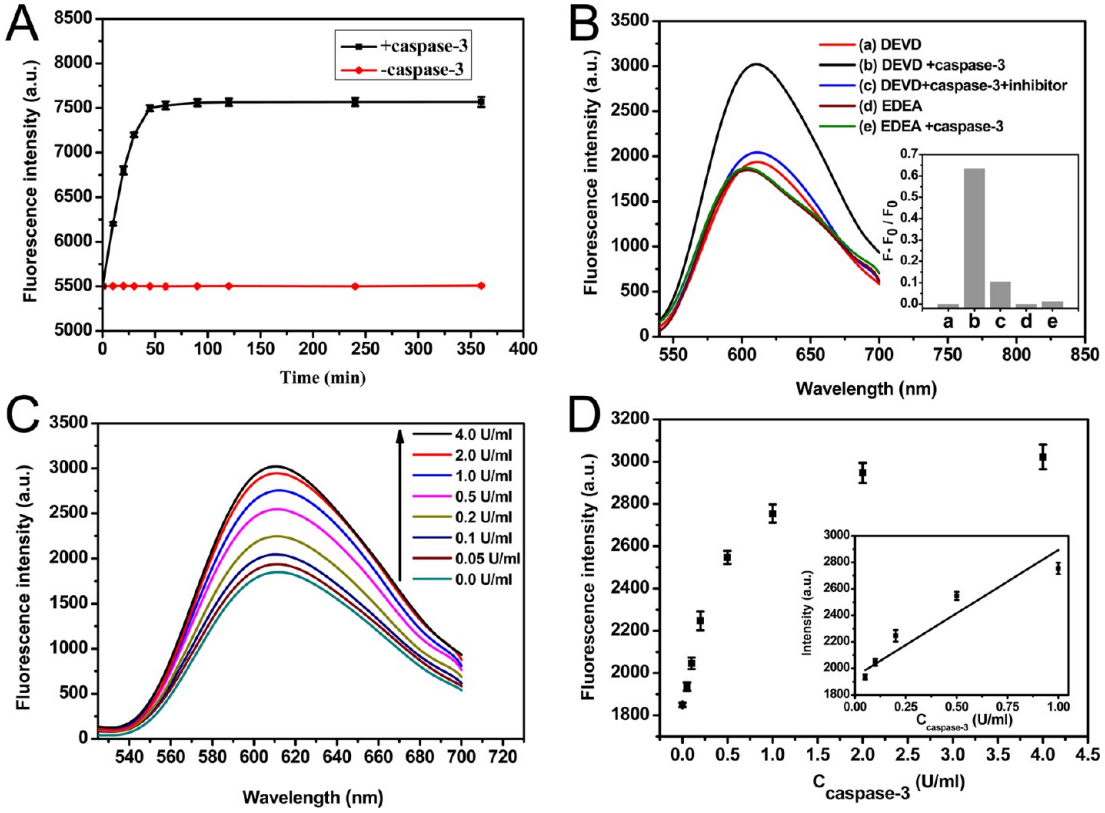

Figure 4. (A) Fluorescence intensity of the assembled nanohybrids of SiNP-peptide-AuNP with and without caspase-3 as function of incubation time. (B) Fluorescence spectra of the SiNP-peptide (DEVD)-AuNP (a) in the absence of caspase-3, (b) in the presence of caspase-3, (c) in the presence of caspase-3 with caspase-3 inhibitor, and (d) fluorescence spectra of the SiNP-peptide (EDEA)-AuNP in the absence of caspase-3, (e) in the presence of caspase-3. (C) Fluorescence spectra of the SiNP-peptide-AuNP in the presence of various concentrations of caspase-3 following incubation for 2 h. (D) Fluorescence intensity of the assembled nanohybrids of SiNP-peptide-AuNP as a function of caspase-3 concentration. Data were presented as average ± SD from three independent measurements.

technique,[51] and fluorescence spectroscopy.[38,52−55] A nanosensor platform to monitor the caspase cascade in apoptotic cells have been developed basing on a nanoquencher that is generated by incorporating a series of dark quencher into SiNPs.[55] In comparison, the detection sensitivity of the nanohybrid system was found to be higher or comparable than those of other DEVD-containing peptide-based FRET systems.[13,38,47−55] Compared to those molecular fluorophore-quencher systems,[47−49] longer enzymatic reaction time was needed for the nanohybrid system to obtain stable signals, possibly because of the steric hindrance. However, as a new sensing strategy, the nanohybrid FRET system has already demonstrated its capabilities in bioanalysis and biodection.

As designed, the fact that the target protease cleaves the specific peptide linker between nanocomponents formed the basis of the SiNP-peptide-AuNP nanohybrid sensing system. Therefore, high selectivity of the nanohybrid FRET system is reasonably expected. To evaluate the selectivity of the nanohybrids toward caspase-3, a series of proteases, individual amino acids and proteins, were examined for their possible interference in caspase-3 detection.[11] In this study, typical proteases including papain, thrombin, pepsin, lysozyme, trypsin, as well as caspase-7 have been evaluated for their interference to caspase-3 detection. As shown in Figure 5, no obvious fluorescence recovery was observed for any inspected substances except for caspase-7. Caspase-7 can also recognize and cleave DEVD-containing peptide, resulting in the recovery of the SiNPs fluorescence. However, caspase-3 still displays

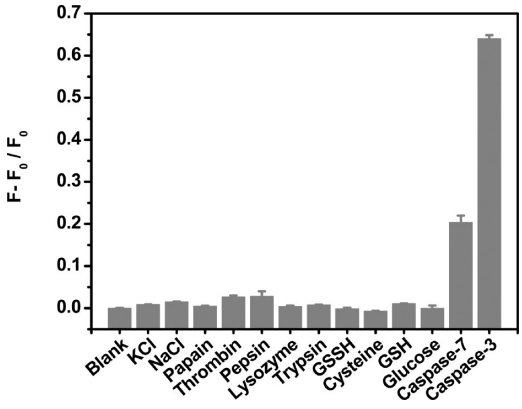

Figure 5. Specificity test for blank and negative control solutions for caspase-3, where F_0 represents the fluorescence intensity of the SiNP-peptide-AuNP, and F is the fluorescence intensity of the nanohybrid plus inspected species.

around 3-fold higher change in $(F - F_0)/F_0$ than caspase-7, which is consistent with previous reports.[47,48] All the results indicated that the peptide linker containing DEVD sequence shows good specificity for caspase-3 cleavage, and suggested that the thus assembled nanohybrid system demonstrated high selectivity toward caspase-3 detection.

To demonstrate the sensing capabilities of the SiNP-peptide-AuNP FRET system in complex biological environment, caspase-3 determination in cell extracts was conducted with

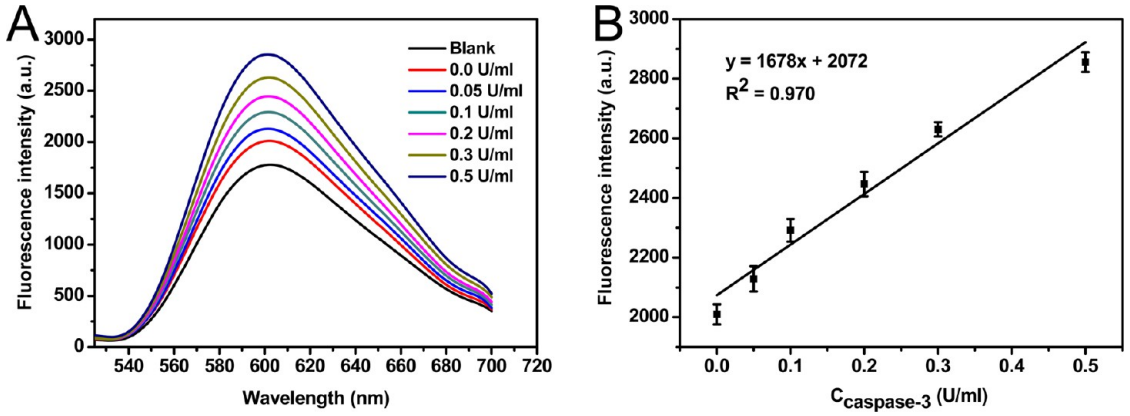

Figure 6. (A) Fluorescence intensity of the assembled nanohybrids of SiNP-peptide-AuNP with various concentrations of caspase-3 (0, 0.05, 0.1, 0.2, 0.3, 0.5 U mL^{-1}). (B) The linear relationship between the fluorescence intensity and the concentration of caspase-3 within the range of 0.05−0.5 U mL^{-1}. Data were presented as average ± SD from three independent measurements.

the nanohybrid system. Using the calibration curve obtained in the aqueous solution (Figure 6A, B), caspase-3 concentration in cell extracts was determined as 0.176 U mL^{-1}. To further validate the determination, standard addition experiments were carried out, and the recoveries were found to be 100.57 and 110.23 with RSD around 3% (Table 2). These results further

Table 2. Analytical Results of the Determination of Caspase-3 in the Cell Extract Sample Using the Assembled Nanohybrids of SiNP-peptide-AuNP

sample	caspase-3 spiked (U mL^{-1})	caspase-3 measured (U mL^{-1})	recovery (%)	RSD (%) (n = 3)
cell extracts	0	0.176		5.4
	0.150	0.344	110.23	3.3
	0.250	0.427	100.57	3.6

demonstrated the potential of the SiNP-peptide-AuNP FRET system in bioanalysis and biodection, which might be significant in disease diagnosis in the future.

CONCLUSION

In summary, the "satellite"-shaped hybrid nanomaterial consisting of $[Ru(bpy)_3]^{2+}$-encapsulated SiNPs and AuNPs has been prepared through peptide-bridged assembly in a controllable way, and has been successfully conditioned for caspase-3 detection through tailoring the FRET efficiency between SiNPs and AuNPs. A peptide which contains recognition sequence DEVD specific for active caspase-3 cleavage was employed to bring SiNPs and AuNPs into FRET proximity through specific molecular recognition. Caspase-3 triggers the cleavage of the link between the two nanoparticles and releases AuNPs from the nanohybrids, inducing the activation of SiNPs to the "ON" state, which forms the basis of caspase-3 determination. The nanohybrid sensor assembled through biomolecule-directed strategy is ultrasensitive and highly selective towards caspase-3 determination, which might be significant in disease diagnosis with proper optimization in the future. In addition, through tailoring the bridging biomolecules or employing other nanocomponents for the targets, it is feasible to develop other nanosensors using the proposed FRET model.

EXPERIMENTAL SECTION

Apparatus. Morphology of the synthesized nanoparticles was examined by transmission electron microscope (TEM, JEOL JEM-1400). A Malvern Zetasizer NanoZS90 instrument was employed to perform DLS measurements. Fluorescent and UV−vis spectra were obtained on a PTI Quanta-Master QM4CW spectrofluorometer and a Beckman DU730 UV−vis spectrometer, respectively.

Synthesis and Functionalization of Fluorescent SiNPs. The fluorescent $[Ru(bpy)_3]^{2+}$-encapsulated SiNPs were synthesized by a water-in-oil reverse micelle method as described in detail elsewhere.[35] Typically, 7.5 mL of cyclohexane, 1.77 mL of Triton X-100, 1.8 mL of hexanol, and 0.34 mL of H_2O were stirred for 20 mins to generate the microemulsion system. Then, 80 μL of 0.1 M $[Ru(bpy)_3]^{2+}$ and 100 μL of tetraethoxy orthosilicate (TEOS) was added to the mixture. After being stirred for 30 min, 60 μL of aqueous ammonia was added to the mixture to initiate silica polymerization. After the reaction proceeded for 24 h, 50 μL of TEOS and 50 μL of carboxyethylsilanetriol sodium salt (CTES) were then added to functionalize SiNPs with carboxylic groups (SiNP-COOH). The reaction was allowed to continue for 24 h. Finally, acetone was added to destabilize the microemulsion system. The fluorescent SiNPs were isolated via centrifugation and washed in sequence with ethanol and D.I. water to remove any surfactant and unreacted reactants.

To functionalize SiNPs with avidin, carbodiimide chemistry was employed as described in detail elsewhere.[36] Briefly, 0.1 g of SiNP-COOH was suspended in 2 mL of 0.1 M 2-(N-morpholino) ethanesulfonic acid (MES, pH 5.5) buffer containing 5 mM N-hydroxysuccinimide (NHS) and 2 mM 1-ethyl-3-(3-dimethyl-aminopropyl) carbodiimide (EDC) to activate carboxylic groups. After 30 min, the SiNPs were centrifuged followed by washing with 10 mM phosphate buffer (PBS, pH 7.4), and then re-suspended in 1.5 mL PBS. Then, 100 μL of 1 mg mL^{-1} avidin solution was added into SiNPs with activated carboxylic groups, and the mixture was allowed to react at room temperature for another 3h under gentle shaking. Avidin-modified SiNPs (SiNP-avidin) were washed with 10 mM PBS (pH 7.4) and then resuspended in quenching solution (40 mM Tris-HCl with 0.05% (w/v) BSA) for 1 h to block free carboxylates. SiNP-avidin was purified by alternately centrifugating and resuspending in PBS with 10 mg mL^{-1} BSA and stored at 4 °C until use.

Synthesis and Functionalization of AuNPs. Aqueous dispersions of citrate-stabilized AuNPs were prepared by the citrate reduction of chloroauric acid as described in detail elsewhere.[22,37] Briefly, 100 mL of 1 mM $HAuCl_4$ solution was heated to boiling under vigorous stirring, followed by quickly adding 10 mL of 38.8 mM trisodium citrate solution. The reaction was allowed to continue for another 20 min. Then, the solution was cooled to room temperature and filtered by 0.45 μm cellulose acetate (CA) membranes. The as-prepared AuNPs were stored at 4°C in the refrigerator for further use.

dx.doi.org/10.1021/am401935y | ACS Appl. Mater. Interfaces 2013, 5, 6494−6501

Biotinylated peptides (target sequence: Gly-Gly-Gly-Asp-Glu-Val-Asp-Gly-Gly-Cys; control sequence: Gly-Gly-Gly-Glu-Asp-Glu-Ala-Gly-Gly-Cys) were purchased from GL Biochem. Ltd. (Shanghai, China) and conjugated to AuNPs via the Au−S bond as described in detail elsewhere.[38] Briefly, 1 mL of 1 mg mL^{-1} peptides solution and 1 mL of 50 μg mL^{-1} SH-PEG_{1000} was added to 20 mL of 0.95 nM AuNPs, followed by incubation for 24 h. Excess peptides and SH-PEG_{1000} were then removed by centrifugation at 13 000 g for 30 min. The resultant peptide-modified AuNPs (AuNP-peptide) were washed with DI water and redispersed in PBS (50 mM, pH 7.4).

Assembly of the SiNP-peptide-AuNP Nanohybrid. Assembly of the designed hybrid nanomaterial was achieved through the highly specific biomolecular recognition of avidin-biotin.[38] Typically, biotinylated peptide-conjugated AuNPs with various concentrations (final concentrations: 0, 1.0, 2.0, 3.5, 4.5, 5.5, 7.5, and 9.5 nM) were added to 0.4 μg mL^{-1} avidin-conjugated SiNPs to initiate the assembly in 1.0 mL of assay solution. The mixture was left to react for 4 h. The resulting nanohybrids were isolated by centrifugation at 5000 rpm for 10 min, and then washed with DI water and redispersed in HEPES buffer (50 mM, pH 7.4).

Sensing Application of the SiNP-peptide-AuNP Nanohybrid. For caspase-3 detection, the hybrid conjugates SiNP-peptide-AuNP with a weak fluorescence was used as a sensing system. 1.12 μg nanohybrid were incubated with recombinant caspase-3 (final concentrations: 0, 0.05, 0.1, 0.2, 0.5, 1.0, 2.0, 4.0 U mL^{-1}) in 1.0 mL of assay buffer (pH 7.4, 50 mM HEPES, 100 mM NaCl, 1 mM EDTA, 10% v/v glycerol and 0.1% v/v CHAPS) for 2 h at 37°C.[38] In the first control experiment, the caspase-3 inhibitor Ac-DEVD-CHO was added into SiNP-peptide-AuNP nanohybrid system in the presence of caspase-3. In another control experiment, the nanohybrids assembled through non-specific sequence-containing peptide (EDEA) were incubated with and without recombinant caspase-3 (4.0 U mL^{-1}). To evaluate the selectivity of the SiNP-peptide-AuNPs nanohybrids toward caspase-3, a series of proteases, individual amino acids and proteins, were tested for their possible interference in caspase-3 detection. The fluorescence spectra were recorded with an excitation of 451 nm at 37 °C at appropriate time intervals.

Caspase-3 determination with the nanohybrid sensor was also conducted in cell extracts.[56] HepG2 cells were obtained from American Type Culture Collection (ATCC, Manassas, VA, USA), and were cultured in DMEM medium (supplemented with 15% fetal bovine serum) at 37°C in a humidified 5% CO_2 atmosphere. 1.0×10^6 cells were collected in the exponential phase of growth, and were then dispensed in an EP tube. After washed twice with ice-cold PBS, cells were re-suspended in 200 μL of ice-cold CHAPS buffer. The suspension was subjected to sonication in an ice bath (Misonix sonicator S-4000 amplitude set at 70%) for 30 min and centrifuged at 12000 rpm for 20 mins. The suspension was carefully transferred to a new EP tube, and was used immediately for caspase-3 detection after 10-fold dilution with assay buffer or stored at −70 °C. The same experimental conditions and fluorescence measurement procedures as in aqueous solution was followed.

■ ASSOCIATED CONTENT

Ⓢ Supporting Information

TEM image of SiNP-avidin and AuNP-biotinylated peptides. This material is available free of charge via the Internet at http://pubs.acs.org.

■ AUTHOR INFORMATION

Corresponding Author

*E-mail: yichq@mail.sysu.edu.cn. Tel/Fax: (86)-20-39342380.

Notes

The authors declare no competing financial interest.

■ ACKNOWLEDGMENTS

The financial support from the National Scientific Foundation of China (NSFC 21171038, 31100723), Guangdong Natural Science Foundation (S2011040001778), Funding Scheme of Guangdong Provincial Key Laboratory of Sensing Technology and Biomedical Instruments (2011A060901013), and the Research Grants Council of the Hong Kong Special Administrative Region (CityU161310) is gratefully acknowledged.

■ REFERENCES

(1) Jiang, K. Y.; Eitan, A.; Schadler, L. S.; Ajayan, P. M.; Siegel, R. W. *Nano Lett.* **2003**, *3*, 275−277.
(2) Schulz-Drost, C.; Sgobba, V.; Gerhards, C.; Leubner, S. *Angew. Chem., Int. Ed.* **2010**, *49*, 6425−6429.
(3) Osterloh, F. E.; Martino, J. S.; Hiramatsu, H.; Hewitt, D. P. *Nano Lett.* **2003**, *3*, 125−129.
(4) Banerjee, S.; Wong, S. S. *J. Am. Chem. Soc.* **2003**, *125*, 10342−10350.
(5) Choi, J. S.; Jun, Y. W.; Yeon, S. I.; Kim, H. C.; Shin, J. S.; Cheon, J. *J. Am. Chem. Soc.* **2006**, *128*, 15982−15983.
(6) Kang, H.; Clarke, M. L.; Tang, J. Y.; Woodward, J. T.; Chou, S. G.; Zhou, Z. P.; Simpson, J. R.; Walker, A. R. H.; Nguyen, T.; Hwang, J. *ACS Nano* **2009**, *3*, 3769−3775.
(7) Li, F.; Zhang, Z. P.; Peng, J.; Cui, Z. Q.; Pang, D. W.; Li, K.; Wei, H. P.; Zhou, Y. F.; Wen, J. K.; Zhang, X. E. *Small* **2009**, *5*, 718−726.
(8) Zhang, C. L.; Yuan, Y. X.; Zhang, S. M.; Wang, Y. H.; Liu, Z. H. *Angew. Chem. Int. Ed.* **2011**, *50*, 6851−6854.
(9) Dong, H. F.; Gao, W. C.; Yan, F.; Ji, H. X.; Ju, H. X. *Anal. Chem.* **2010**, *82*, 5511−5517.
(10) Wang, Y. H.; Bao, L.; Liu, Z. H.; Pang, D. W. *Anal. Chem.* **2011**, *83*, 8130−8137.
(11) Wang, Y. H.; Shen, P.; Li, C. Y.; Wang, Y. Y.; Liu, Z. H. *Anal. Chem.* **2012**, *84*, 1466−1473.
(12) Wu, S. J.; Duan, N.; Ma, X. Y.; Xia, Y.; Wang, H. G.; Wang, Z. P.; Zhang, Q. *Anal. Chem.* **2012**, *84*, 6263−6270.
(13) Kim, Y. P.; Oh, Y. H.; Oh, E.; Ko, S.; Han, M. K.; Kim, H. S. *Anal. Chem.* **2008**, *80*, 4634−4641.
(14) Li, M. J.; Wang, Q. Y.; Shi, X. D.; Hornak, L. A.; Wu, N. Q. *Anal. Chem.* **2011**, *83*, 7061−7065.
(15) Xue, M.; Wang, X.; Duan, L. L.; Gao, W.; Ji, L. F.; Tang, B. *Biosens Bioelectron.* **2012**, *36*, 168−173.
(16) Zeng, Q. H.; Zhang, Y. L.; Liu, X. M.; Tu, L. P.; Kong, X. G.; Zhang, H. *Chem. Commum.* **2012**, *48*, 1781−1783.
(17) Novak, J. P.; Feldheim, D. L. *J. Am. Chem. Soc.* **2000**, *122*, 3979−3980.
(18) Yi, C. Q.; Liu, D. D.; Yang, M. S. *Curr. Nanosci.* **2009**, *5*, 75−87.
(19) Mcmillan, R. A.; Paavola, C. D.; Howard, J.; Chan, S. L.; Zaluzec, N. J.; Trent, J. D. *Nat. Mater.* **2002**, *1*, 247−252.
(20) Wang, S. P.; Mamedova, N.; Kotov, N. A.; Chen, W.; Studer, J. *Nano Lett.* **2002**, *2*, 817−822.
(21) Mirkin, C. A.; Letsinger, R. L.; Mucic, R. C.; Storhoff, J. J. *Nature* **1996**, *382*, 607−609.
(22) Elghanian, R.; Storhoff, J. J.; Mucic, R. C.; Letsinger, R. L.; Mirkin, C. A. *Science* **1997**, *277*, 1078−1081.
(23) Mucic, R. C.; Storhoff, J. J.; Mirkin, C. A.; Letsinger, R. L. *J. Am. Chem. Soc.* **1998**, *120*, 12674−12675.
(24) Pinto, Y. Y.; Le, J. D.; Seeman, N. C.; Musier-Forsyth, K.; Taton, T. A.; Kiehl, R. A. *Nano Lett.* **2005**, *5*, 2399−2402.
(25) Lee, S. W.; Mao, C. B.; Flynn, C. E.; Belcher, A. M. *Science* **2002**, *296*, 892−895.
(26) Mao, C. B.; Solis, D. J.; Reiss, B. D.; Kottmann, S. T.; Sweeney, R. Y.; Hayhurst, A.; Georgiou, G.; Iverson, B.; Belcher, A. M. *Science* **2004**, *303*, 213−217.
(27) Berry, V.; Saraf, R. F. *Angew. Chem., Int. Ed* **2005**, *44*, 6668−6673.

(28) Rosi, N. L.; Thaxton, C. S.; Mirkin, C. A. *Angew. Chem., Int. Ed.* **2004**, *43*, 5500−5503.
(29) Yang, Z.; Liang, G.; Guo, Z.; Xu, B. *Angew. Chem., Int. Ed.* **2007**, *46*, 8216−8219.
(30) Sapsford, K. E.; Berti, L.; Medintz, I. L. *Angew. Chem., Int. Ed.* **2006**, *45*, 4562−4588.
(31) Wang, L.; Wang, K. M.; Santra, S.; Zhao, X. J.; Hilliard, L. R.; Smith, J. E.; Wu, J. R.; Tan, W. *Anal. Chem.* **2006**, *78*, 646−654.
(32) Santra, S.; Zhang, P.; Wang, K.; Tapec, R.; Tan, W. *Anal. Chem.* **2001**, *73*, 4988−4993.
(33) Meng, H.; Liong, M.; Xia, T.; Li, Z. X.; Ji, Z. X.; Zink, J. I.; Nel, A. E. *ACS Nano* **2010**, *4*, 4539−4550.
(34) Cohen, G. M. *Biochem. J.* **1997**, *326*, 1−16.
(35) Arriagada, F. J.; Osseo-Asare, K. *J. Colloid Interface Sci.* **1999**, *211*, 210−220.
(36) Greg, T. *Bioconjugate Techniques*, 2nd ed.; Academic: New York, 1996; Vol. *219*, p 598.
(37) Yao, H.; Yi, C. Q.; Tzang, C. H.; Zhu, J. J.; Yang, M. S. *Nanotechnology* **2007**, *18*, 015102.
(38) Gao, W.; Ji, L. F.; Li, L.; Cui, G. W.; Xu, K. H.; Li, P.; Tang, B. *Biomaterials* **2012**, *33*, 3710−3718.
(39) Gwenin, V. V.; Gwenin, C. D.; Kalaji, M. *Langmuir* **2011**, *27*, 14300−14307.
(40) Lim, I. S.; Goroleski, F.; Mott, D.; Kariuki, N.; Ip, W.; Luo, J.; Zhong, C. *J. Phys. Chem. B.* **2006**, *110*, 6673−6682.
(41) Nath, N.; Chilkoti, A. *Anal. Chem.* **2002**, *74*, 504−509.
(42) Clapp, A. R.; Medintz, I. L.; Mauro, J. M.; Fisher, B. R.; Bawendi, M. G. H. *J. Am. Chem. Soc.* **2004**, *126*, 301−310.
(43) Zhang, C. Y.; Yeh, H. C.; Kuroki, M. T.; Wang, T. H. *Nat. Mater.* **2005**, *4*, 826−831.
(44) Rastogi, S. K.; Pal, P.; Aston, D. E.; Bitterwolf, T. E.; Branen, A. L. *ACS Appl. Mater. Interfaces* **2011**, *3*, 1731−1739.
(45) Kim, K.; Lee, M.; Park, H.; Kim, J. H.; Kim, S.; Chung, H.; Choi, K.; Kim, I. S.; Seong, B. L.; Kwon, I. C. *J. Am. Chem. Soc.* **2006**, *128*, 3490−3491.
(46) Hengartner, M. O. *Nature* **2000**, *407*, 770−776.
(47) Zhou, Z. J.; Tang, Y. L.; Whitten, D. G.; Achyuthan, K. E. *ACS Appl. Mater. Interfaces* **2009**, *1*, 162−170.
(48) Shi, H. B.; Kwok, R. T.; Liu, J. Z.; Xing, B. G.; Tang, B. Z.; Liu, B. *J. Am. Chem. Soc.* **2012**, *134*, 17972−17981.
(49) Suzuki, M.; Tanaka, S.; Ito, Y.; Inoue, M.; Sakai, T.; Nishigaki, K. *Biochim. Biophys. Acta* **2012**, *1823*, 215−226.
(50) Pan, Y. L.; Guo, M. L.; Nie, Z.; Huang, Y.; Peng, Y.; Liu, A. F.; Qing, M.; Yao, S. Z. *Chem. Commun.* **2012**, *48*, 997−999.
(51) Zhang, J. J.; Zheng, T. T.; Cheng, F. F.; Zhu, J. J. *Chem. Commum.* **2011**, *47*, 1178−1180.
(52) Boeneman, K.; Mei, B. C.; Dennis, A. M.; Bao, G.; Deschamps, J. R.; Mattoussi, H.; Medintz, I. L. *J. Am. Chem. Soc.* **2009**, *131*, 3828−3829.
(53) Wang, H.; Zhang, Q.; Chu, X.; Chen, T.; Ge, J.; Yu, R. *Angew. Chem., Int. Ed.* **2011**, *50*, 7065−7069.
(54) Prasuhn, D. E.; Feltz, A.; Blanco-Canosa, J. B.; Susumu, K.; Stewart, M. H.; Mei, B. C.; Yakovlev, A. V.; Louko, C.; Mallet, J.; Oheim, M.; Dawson, P. E.; Medintz, I. L. *ACS Nano* **2010**, *4*, 5487−5497.
(55) Huang, X.; Swierczewska, M.; Choi, K. Y.; Zhu, L.; Bhirde, A.; Park, J.; Kim, K.; Xie, J.; Niu, G.; Lee, K. C.; Lee, S.; Chen, X. *Angew. Chem., Int. Ed.* **2012**, *51*, 1625−1630.
(56) Li, Y. P. *Microchim. Acta.* **2012**, *177*, 443−447.